TECHNICAL PAPER

Evaluation of tool wear in high-speed face milling of Al/SiC metal matrix composites

Reza Ghoreishi[1] · Amir H. Roohi[2] · Amir Dehghan Ghadikolaei[3]

Abstract
In recent years, a new generation of composite materials has been introduced as metal matrix composites (MMCs) in order to simultaneously provide higher strength and stiffness. Industrial interests resulted in deep investigations and researches on machinability of MMCs and especially in the field of high-speed machining. High-speed machining processes offer a higher machining efficiency and reduced cost of the process, which made them the process of interest in many manufacturing industries. However, matrix reinforcement by addition of hard particle phases to the MMCs significantly increases machining difficulty, tool wear, surface quality deterioration and overall fabrication costs. In the current research, the cutting speed, feed rate, depth of cut, presence of cryogenic coolant and their effect on the tool wear of high-speed machining of Al/SiC MMC reinforced with 15 wt% SiC particles have been investigated. The results have shown that silicon carbide particles in the aluminum matrix cause a severe tool wear. However, the severity of tool wear has decreased by applying a cryogenic cooling.

Keywords Metal matrix composites (MMCs) · High-speed machining · Cryogenic cooling · Aluminum/silicon carbide (Al/SiC) · Tool wear

1 Introduction

High-speed machining is an interesting process due to its high material removal rate (MMR), low cutting forces, high surface quality and lower processing time, while it increases the manufacturing efficiency [1]. In addition, high wear resistance, thermal stability, strength/weight ratio and corrosion resistance of MMCs compared to the original matrix materials increased their applications in various industries [2]. Rawl et al. [3] have introduced huge benefits of MMCs in automotive and aerospace applications thanks to their

✉ Amir H. Roohi
Amir.roohi@qiau.ac.ir

1 Department of Mechanical Engineering, Semnan University, Semnan, Iran

2 Department of Mechanical Engineering, Faculty of Industrial and Mechanical Engineering, Qazvin Branch, Islamic Azad University, Qazvin, Iran

3 School of Mechanical, Manufacturing and Industrial Engineering, Oregon State University, Corvallis, OR 97331, USA

lightweight and reliable mechanical properties. Many metals can be used as matrix and reinforcement particles that increase flexibility in designing an application of MMC with the desired properties. These materials include copper, tungsten, magnesium, titanium, nickel, iron, etc. [4].

Numerous studies have investigated the properties of MMCs in depth. Gireesh et al. [5] have investigated the mechanical properties of reinforced Al MMC. They have reported enhanced mechanical properties such as hardness, tensile and impact strength. Voyiadjis et al. [6] have studied inelasticity and micromechanics of MMCs. However, aluminum-based MMCs with SiC and alumina (Al_2O_3) reinforcement particles are gaining more attention due to availability and superior mechanical properties. In addition, Al/SiC MMCs demonstrate good thermal stability in heat transfer applications [7, 8]. Similar to many difficult-to-cut alloys and materials (i.e., nickel-based superalloys, NiTi alloys, tungsten, etc.), MMCs are challenging materials when it comes to machining [9]. Machining of MMCs is investigated in depth by many researchers as it is one of the most crucial steps of fabricating these parts. Pramanik et al. [10] have studied cutting force prediction in the machining of Al-based MMC with SiC and alumina reinforcement particles. They have calculated the chip formation force

using Merchant's analysis and consequently have predicted the matrix plowing and particle fracture forces by slip line field and Griffith theories, respectively. Comparing the presented experimental and prediction results, it appears that the implemented theories explain the material removal mechanism in MMCs. Ge et al. [11] have investigated the high-speed machining of Al/SiC MMC by implementing 600–1200 m/min cutting force with a polycrystalline diamond (PCD) tool in order to show the effect of cutting speed on cutting forces during the process. They have reported that with an increased cutting speed in the selected range, the cutting forces decrease, while with an increase in the radial depth of cut (DOC) and feed rate, the cutting forces tend to increase. They have also mentioned that with dispersing smaller reinforcement particles and increasing their overall weight percent in the matrix, the cutting forces increase. Heo et al. [12] have presented automated selection of feed, depth/width and speed of cuts by involving machine constraints (i.e., chatter stability, power and torque) in pocketing process. With respect to machine limitations, they have utilized genetic search algorithms to find spindle speeds, depth/width of cuts and feed rates in the optimal machining conditions. Ke et al. [13] have implemented nitrogen gas at a pressure of 0.7 MPa in high-speed machining of Ti–6Al–4V alloys in order to prevent chip burning and at the same time, removing them from the machining zone during the machining process. They have reported a less surface hardening of the materials in the tool–workpiece interaction which resulted in lower tool wear and surface roughness. Velasquez et al. [14] have investigated high-speed orthogonal milling of Ti–6Al–4V using carbide tools with diamond buildup edge and its effect on subsurface crystallography and residual stresses. The tool specifications of their study were rake angle of 0°, clearance angle of 7°, cutting speed of 20–660 mm/s and feed rate of 0.12 mm/rev. Josyula et al. [15] have studied the effects of applying pressurized LN_2 (as a coolant) in the cutting process of Al–5%TiCP samples. They observed that using the cryogenic cooling condition, compared to dry cutting, enhances the machining conditions (such as surface roughness and tool wear) as well as a reduction in the buildup edge formation. Ghoreishi et al. [16] have investigated high-speed machining of Al/SiC MMCs (up to 2500 m/min) in the presence of cryogenic CO_2 coolant and reported a 19–23% surface roughness improvement and 3–8% increase in cutting forces. In another study, Josyula et al. [17] have investigated the effects of using atomized-cryogenic-liquid spray machining technique for fabrication of high-quality Al–TiCp composites. Both microstructural and mechanical investigations show an improved results, no metallic reaction during the process and reduced progressive tool wear and manufacturing cost, as well. Kumar et al. [18] have studied the surface roughness in turning of Al 7075 MMC (7 wt% SiC/3 wt% graphite and 10 wt% SiC)

using PCD tools with rake angle of 0°, clearance angle of 7° and nose radius of 0.4 mm. They have reported that the surface roughness of the first group is lower, and they have validated the experimental results by the response surface method (RSM) and neural network analysis (NNA), claiming that the feed rate had the most significant effect. In a different study by Han et al. [19], they have investigated milling of high volume fraction Al/SiC MMC (with 65% SiC particles) with PCD tools with different tool edges (sharp and chamfered) and grain sizes at a constant spindle speed of 10,000 rpm. They have reported that an increase in feed rate and depth of cut resulted in increased and decreased surface roughness, respectively. They have also mentioned no significant difference in the results of two different tool geometries. In a similar study by Bian et al. [20], they have investigated the effect of micromilling of high volume fraction Al/SiC (with 65% SiC particle) on surface roughness and tool wear of a monocrystalline diamond cutting tool. They have conducted the experiments at a constant spindle speed of 1000 rpm, 1–2 and 2–4 μm/tooth of feed rate and depth of cut, respectively. From their experimental results, they have concluded that it is possible to achieve a mirror finish surface with surface roughness of 0.1 μm Ra, but the surface shows many micro-cracks and fracture areas. In addition, they have reported a high flank wear in the cutting tool that might be a result of chemical transformation of diamond to graphite. In a recent work by Teng et al. [21], they have numerically and experimentally compared the cutting mechanism of micro- and nanoparticle-reinforced Al/SiC MMC. The experimental conditions were cutting speed of 125.64 m/min, depth of cut of 30 μm and feed rate of 4 μm/tooth. The SiC particle sizes were 10 and 0.2 μm for micro- and nano-sized particles, respectively. They have reported that the having parts with smaller particle reinforcement, a higher surface quality is achieved and the stress distribution of those parts is more homogeneous as there is less particle fracture.

Regarding the growing applications of MMCs in different industries, it becomes important to have a comprehensive understanding of these materials. The focus of the current study is on high-speed machining of Al/SiC MMC reinforced with 15 wt% SiC particles and machining conditions of 1000–2500 m/min cutting speed, 0.25–2 mm depth of cut and 0.01–0.1 mm/tooth feed rate. A deep analysis of the results of the experiments has been performed in order to investigate the effect of different process parameters on the tool wear rates and values of the machined Al/SiC specimens. In addition, CO_2 coolant and its effect on tool wear have been investigated.

2 Materials and methods

The Al/SiC MMC used in this study was made from A356.0-T6 Al alloy due to its interesting physical and mechanical characteristics (such as high strength to weight ratio, brilliant corrosion resistance and high machinability). The chemical analysis of the used Al is reported in Table 1, which is performed by the authors in the metallurgy laboratory. SiC particles were used as the reinforcement with the mesh size of $-200/+320$ (50–74 μm) in order to achieve a higher wettability. The weight percent of the reinforcement portion was selected to be 15 wt% to prevent agglomeration and rejection of the particles to the slug, during mixing and casting [22]. Vortex casting was implemented for fabrication of the ingots as it has lower process cost and it is easier to perform. The general process is that the reinforcement particles are added to a melt pool and mixed mechanically prior to pouring into a preheated steel mold. The casting process in detail starts with melting a portion of the prepared Al in a graphite crucible in a temperature of 725 °C reducing the temperature to 675 °C and the addition of 0.5 wt% Mg to increase the wettability properties of the melt [23]. In the next step, the preheated SiC particles (preheated at 1000 °C) are added to the melt pool, and the temperature is increased to 725 °C in order to have a proper melt viscosity during the mixing process. Then, the graphite mixer continues working for 5 more minutes to ensure the highest homogeneity. After the mix is ready, it is poured into a preheated steel cavity and undergoes a constant hydraulic pressure of 40 MPa until it reaches the room temperature [24]. Finally, samples in a size of $40 \times 60 \times 120$ mm^3 were made with the consideration of a surface area smaller than that of the cutting tool. As it can be seen from metallography images in Fig. 1, the SiC particles are homogeneously dispersed in the Al matrix.

The machining process was conducted using a three-axis Dah Lih CNC machine model VMC1050 and a FANUC controller with a maximum of 15,000 rpm rotational speed. The face milling tool Octomill 220.43-05A and the CVD-coated Ti(C, N)–Al$_2$O$_3$ grade T350 M cutting inserts were provided by SECO. The outer tool diameter was 63 mm with six screw-tight insert supports that could provide a maximum of 3.5 mm depth of cut. A high-pressure CO$_2$ capsule was used to provide a cryogenic cooling mechanism by jetting CO$_2$ to the machining area at a pressure of 3 bar and mass flow of 6 g/s. The position of the cooling nozzle was adjusted automatically, relative to the cutting point. The image of the experimental setup is
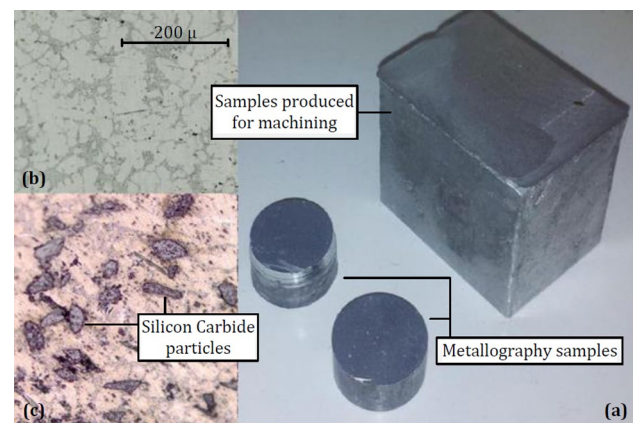
Fig. 1 **a** Images of the samples; **b** optical microscopy of the A356.0-T6 Al alloy; and **c** optical microscopy of the Al/SiC MMC

shown in Fig. 2. A Dino-Lite digital microscope was used to measure the tool wear at the tip of the cutting inserts. Each of the used inserts had eight cutting edges that two of them were involved in a single cutting process. After each cutting experiment, the tools were rotated 180 degrees in order to introduce the intact cutting edges to the surface of the workpiece. The major and minor edges of the tool are illustrated in Fig. 3. The two cutting edges were responsible for the main cutting process and a consequent finishing process in the machining area. In order to clean the used inserts from any Al residues, a HCl (50%)–HNO$_3$(4%)–HF (3%) etchant was used [25].

3 Results and discussion

In general, adjustable machining parameters such as spindle speed, feed rate, depth of cut, tool material/geometry/cutting angles and coolant type are known as input parameters that can affect the output parameters such as geometrical tolerance, surface roughness, tool wear and machining time. It is worth mentioning that the goal of all the current experiments is to remove 14 cm^3 of the material during the experimentations. The set of continuous parameters of the experimental work consists of velocity (m/s), feed rate (mm/tooth) and depth of cut (mm) with five different levels in the design of experiments (i.e., response surface methodology) set as $-\alpha, -1, 0, +1$ and $+\alpha$. On the other hand, the cooling parameter is set as a discrete parameter with two levels of -1 and $+1$, which means there is an active cooling in the machining process, while the level is $+1$ and the machining is done in the absence of the cooling medium, while the design level is -1. All the discussed levels

Table 1 Chemical analysis of the A356.0-T6 alloy used in preparing the Al/SiC MMC (wt%)

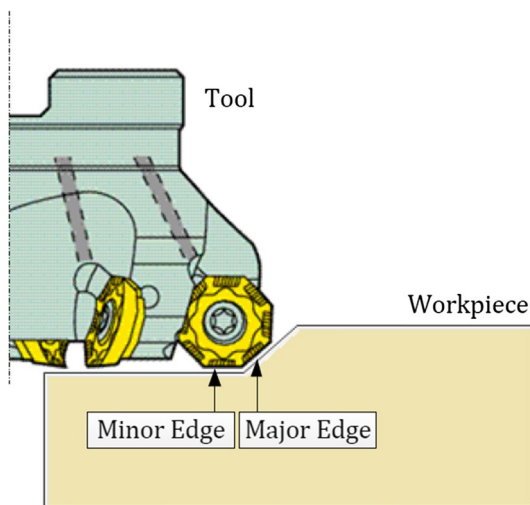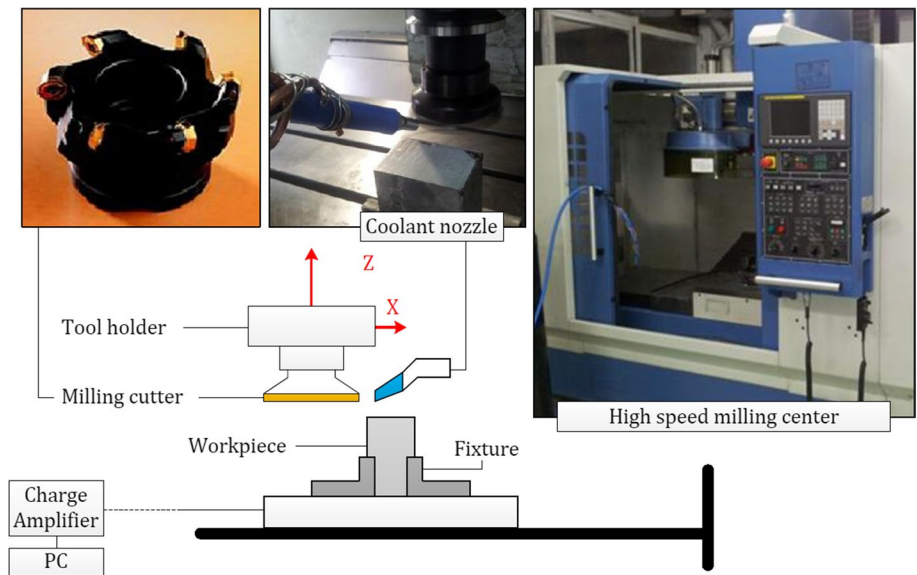| Al base metal	Si 6.65	Fe 0.18	Cu 0.0306	Mn 0.0131	Mg 0.385	Cr 0.0016
Ni 0.0069	Zn 0.0406	Ti 0.0077	Be 0.00003	Ca 0.0011	Co < 0.0002	Na < 0.00019
P < 0.0005	Pb < 0.0026	Sb < 0.0001	Sn < 0.0004	Sr < 0.00005	V 0.0168	Zr 0.00048

Fig. 2 Setup for experiments

Fig. 3 Major and minor edges of the cutting tool

are presented in Table 2. In addition, the order of the experiments and the obtained results are listed in Table 3.

Based on indirect tool failure criterion, a drop in surface quality and geometrical tolerance of the workpiece and also an increase in machining forces (regarding the defined surface roughness and geometrical tolerance) indicate the end

of tool life. As the results show, the tool wear in the minor cutting edge was less than the major one as the minor edge provided the final surface roughness, while the major cutting edge was in charge of rough machining. Thus, the tool wear was considerably high in the major cutting edge and even it was completely worn away in some experiments; the results of tool wear in the minor cutting edge were taken into account for assessing the tool–workpiece interaction. The reasons for high tool wear in the major cutting edge were excessive heat generation due to a high load of machining and the abrasive SiC particles that have a high mechanical stability in front of the cutting forces exerted by the cutting tool. These particles are mainly used in abrasive machining and finishing of materials thanks to their high stiffness and hardness [26, 27]. Also, it is known that coatings increase wear/corrosion resistance of substrates [28]. As a result, it is recommended to use CVD-coated tools in order to have a longer tool life and enough time span to investigate the effect of various machining parameters on tool–workpiece interaction. In addition, there is always a chance of burr formation on the surface of the machined materials. Burrs are plastic-deformed portion of materials that reduce part accuracy and need to be removed from the fabricated parts for a better functionality. Figure 4 shows the burr formation in the samples #26 and #29 from Table 3. Sections "a" and

Table 2 Upper- and lower-level values of the machining parameters

Input variables	Kind of variables	Coded levels	Actual levels				
Cutting speed (m/min)	Numeric	$(-\alpha, -1, 0, +1, +\alpha)$	1000	1304	1750	2196	2500
Feed rate (mm/tooth)			0.01	0.028	0.055	0.082	0.1
Depth of cut (mm)			0.25	0.6	1.13	1.65	2
Coolant	Categorical	$(-1, +1)$	Dry non-coolant			CO_2	

Table 3 List of experiments and their obtained results

#	Cutting speed (m/min)	DOC (mm)	Feed rate (mm/tooth)	Coolant	Tool wear (mm)
1	1304	0.6	0.028	–	1.121
2	2196	0.6	0.028	–	1.621
3	1750	1.13	0.1	–	1.223
4	1750	1.13	0.055	–	0.976
5	1304	1.65	0.082	CO_2	0.757
6	2500	1.13	0.055	CO_2	0.954
7	1304	0.6	0.028	CO_2	0.904
8	1750	1.13	0.01	–	1.876
9	2196	0.6	0.082	–	1.55
10	2196	1.65	0.028	CO_2	0.824
11	1750	1.13	0.055	–	1.617
12	1750	0.25	0.055	–	1.761
13	2196	0.6	0.028	CO_2	1.211
14	1750	1.13	0.055	CO_2	1.026
15	1750	1.13	0.055	CO_2	0.937
16	1750	1.13	0.1	CO_2	1.081
17	1750	1.13	0.055	–	1.263
18	1750	1.13	0.055	–	1.153
19	1750	1.13	0.055	CO_2	1.433
20	1304	1.65	0.028	–	0.814
21	2196	1.65	0.028	–	0.987
22	1750	1.13	0.055	CO_2	0.982
23	2196	1.65	0.082	CO_2	0.757
24	1750	1.13	0.055	–	0.926
25	1304	1.65	0.082	–	0.948
26	1000	1.13	0.055	–	1.521
27	2196	1.65	0.082	–	1.013
28	2500	1.13	0.055	–	1.27
29	1000	1.13	0.055	CO_2	1.234
30	1304	1.65	0.028	CO_2	0.668
31	1750	1.13	0.055	CO_2	0.793
32	1750	0.25	0.055	CO_2	1.424
33	1750	1.13	0.055	CO_2	0.898
34	1750	2	0.055	–	0.765
35	1750	2	0.055	CO_2	0.845
36	1304	0.6	0.082	–	1.07
37	1750	1.13	0.01	CO_2	1.502
38	1304	0.6	0.082	CO_2	1.142
39	2196	0.6	0.082	CO_2	0.757
40	1750	1.13	0.055	–	1.106

"b" show the surface of the samples machined with (#29) and without (#26) CO_2 coolant, respectively. Figure 5 represents the tool wear in the major and minor cutting edges of the tool in experiment #29. The upper and lower images represent the tool wear after the first pass of machining and after the machining experiment, respectively. Regardless of

the cooling conditions, the rest of the process parameters (i.e., $V_f = 0.055$ mm/tooth, $a_p = 1.13$ mm and $V_c = 1000$ m/min) were the same.

## 3.1 Analysis of experimental results

The correlations between the input parameters and the obtained tool wear are presented in Table 4 as a general equation and four distinct equations for each input parameter. Indices A, B, C and D are representing the cutting speed, depth of cut, feed rate and cooling. The continuous values vary between $\pm \alpha$, where α is calculated as 1.682 in this study. In addition, the discrete values are either $+1$ or -1.

Based on the literature, one of the major reasons of tool wear is adhesion of workpiece material to the tool coating layer that mostly takes place at elevated machining temperatures. If this adhesion force is larger than the bonding between the tool material and its coating layer, the rate of tool wear increases dramatically. The other reason for severe tool wear can be high mechanical and thermal stresses during the machining processes [29, 30]. Figure 6 represents the relation between cutting speed and tool wear in the center point in dry mode with the same trend toward less and more tool wear values. Considering Fig. 6, sole cutting speed does not increase the tool wear rate in the machining of a certain volume of material by itself (Eq. 2). The graph explains that in two different cutting speeds, the tool wear seems to be in the same range, but it is worth mentioning that in a higher cutting speed, compared to the one with lower cutting speed, the machining process finishes faster, resulting in producing more heat and mechanical stresses. As mentioned above, these are the main factors in determining the rate of tool wear in a specific machining process. As an instance, a process with cutting speed of 2500 m/min gives tool wear rates more than 2.5 times of the same process with a cutting speed of 1000 m/min. Figure 7 represents the relation between the depth of cut and the tool wear (obtained from Eq. 3) during the machining process in the center point and in a dry mode. Increasing the depth of cut in machining decreases the process time and as a result decreases the contact time between the tool and the workpiece, which lead to a decrease in tool wear (in the order of almost two, i.e., $1.63/0.88 = 1.85$). However, regarding Fig. 7, this increase in depth of cut imposes an almost five times greater tool wear rate in the machining process ($8/1.85 = 4.3$). In fact, increasing the depth of cut from 0.25 to 2 mm has reduced the machining time up to eight times (as it is mentioned that the machining removal volume is constantly equal to 14 cm^3), while the tool wear has decreased less than two times. Figure 8 shows the relation of tool wear and the feed rate based on Eq. 4 in the center point in dry mode machining. Similar to the effect of increase in the depth of cut, increasing the feed rate reduces the machining time. As a

Fig. 4 Burr formation in the experiments #29 and #26 from Table 3: **a** with coolant (#29) and **b** without coolant (#26)

(a)　　　　　　　　(b)

Fig. 5 The cutting insert in the experiment #29 from Table 3: **a**, **b** the major and the minor cutting edges in the first machining pass and **c**, **d** the major and the minor cutting edges in the last machining pass
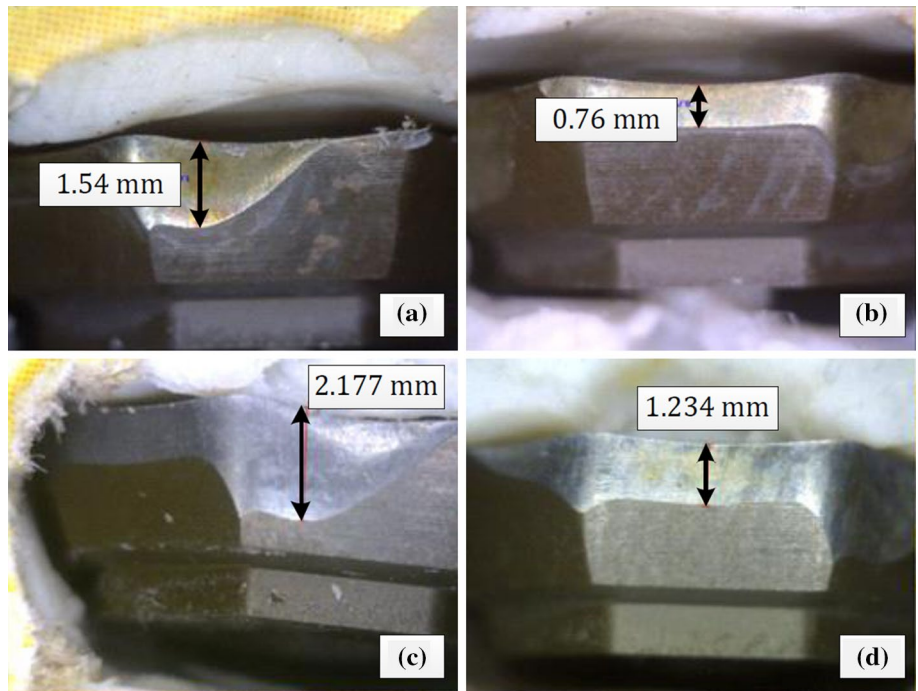
Table 4 Relation between each input parameter and the final tool wear

Equation	Input parameters	Relationship between input parameter and tool wear
1	–	$1/\mathrm{Sqrt(wear)} = 0.97 - 0.006A + 0.084B + 0.021C + 0.047D$
2	Cutting speed	$1/\mathrm{Sqrt(wear)} = (0.97 + 0.084B + 0.021C + 0.047D) - 0.006A$
3	DOC	$1/\mathrm{Sqrt(wear)} = (0.97 - 0.006A + 0.021C + 0.047D) + 0.084B$
4	Feed rate	$1/\mathrm{Sqrt(wear)} = (0.97 - 0.006A + 0.084B + 0.047D) + 0.021C$
5	Coolant	$1/\mathrm{Sqrt(wear)} = (0.97 - 0.006A + 0.084B + 0.021C) + 0.047D$

A: cutting speed, B: depth of cut, C: feed rate and D: coolant

result, the final tool wear was less (from 1.27 to 1.09 mm), although the rate of tool wear was increased to less than seven times (i.e., 8/1.16 = 6.9). Use of coolant maintains the tool temperature and preserves the tool hardness that reduces the tool wear. 16–19% of tool wear reduction was obtained from the experimental results. Figure 9 illustrates the relation between the tool wear and cooling procedure in

machining of an exact volume of material in the center point and in the dry mode. This behavior is obtained from Eq. 5.

3.2 Interactive parameters effect

With the help of interactive graphs, it is possible to predict the tool wear, find the optimum process parameters and minimize
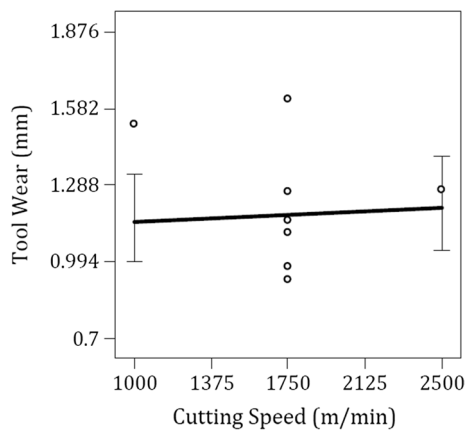
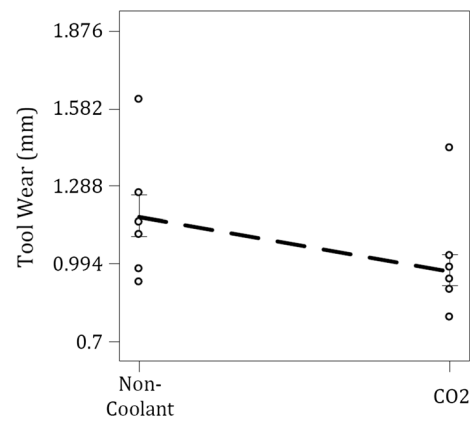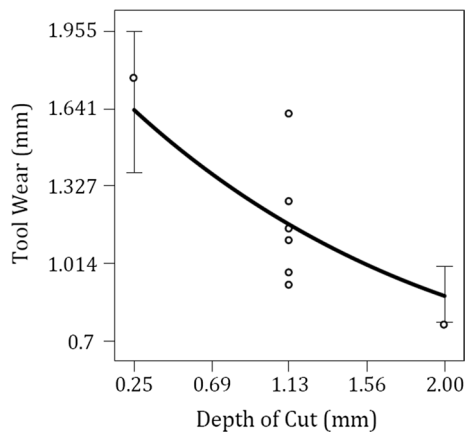**Fig. 6** Interaction of cutting speed–tool wear in the center point

Fig. 7 Interaction of depth of cut–tool wear in the center point

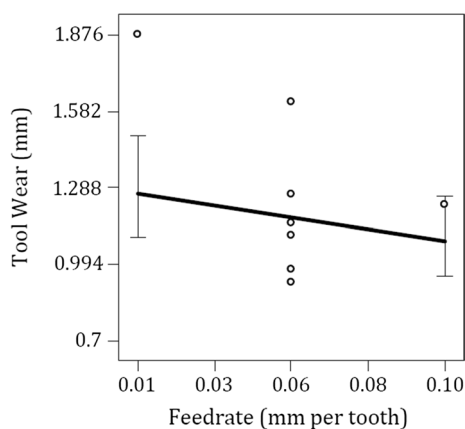**Fig. 8** Interaction of feed rate–tool wear in the center point

Fig. 9 Interaction of coolant–tool wear in the center point

the final tool wear during the machining process. Figure 10 represents the interactive effect of feed rate and depth of cut in different cutting speeds on the tool wear. As it can be seen, variations of cutting speed did not affect the tool wear significantly. Figure 11 shows the interactive effect of cutting speed and feed rate in different depths of cut on the tool wear. It is obvious that increasing the cutting speed in machining an exact volume of material decreased the tool wear. In addition, Fig. 12 shows the interactive effect of cutting speed and depth of cut in different feed rates in machining an exact volume of material. It can be seen that the increase in feed rate reduces the tool wear, but its effect is less significant relative to that of machining depth of cut.

Regarding Figs. 10, 11 and 12, in order to have the minimum tool wear in machining of an exact volume of material, it is important to implement the highest depth of cut and feed rate to have the minimum time of machining and as a result the minimum tool–workpiece interaction. In addition, having a depth of cuts more than 1.5 mm in any given cutting speed and feed rate guarantees a tool wear value less than 1 mm. These changes in the case of having a cryogenic cooling system and maintaining depth of cuts more than 1 mm promise a tool wear value of less than 1 mm in any given cutting speed and feed rate. This finding implies that it is more effective to have a cryogenic cooling system during the machining process. A quantitative evaluation of the experimental and mathematical results shows that in order to have a reliable tool wear, a cutting speed of 1800 m/min, a depth of cut in the range of 1–1.1 mm and a feed rate of less than the mean size of the SiC particles (0.07 mm) are needed other than that the cryogenic cooling condition.
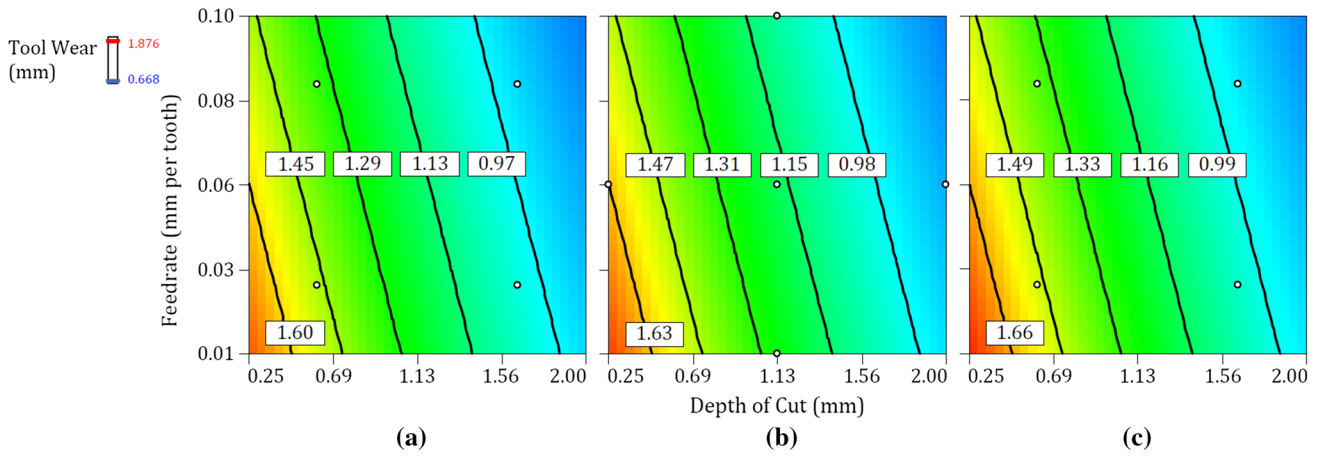
Fig. 10 Interactive effect of feed rate and depth of cut on tool wear at cutting speeds of **a** 1304, **b** 1750 and **c** 2196 m/min
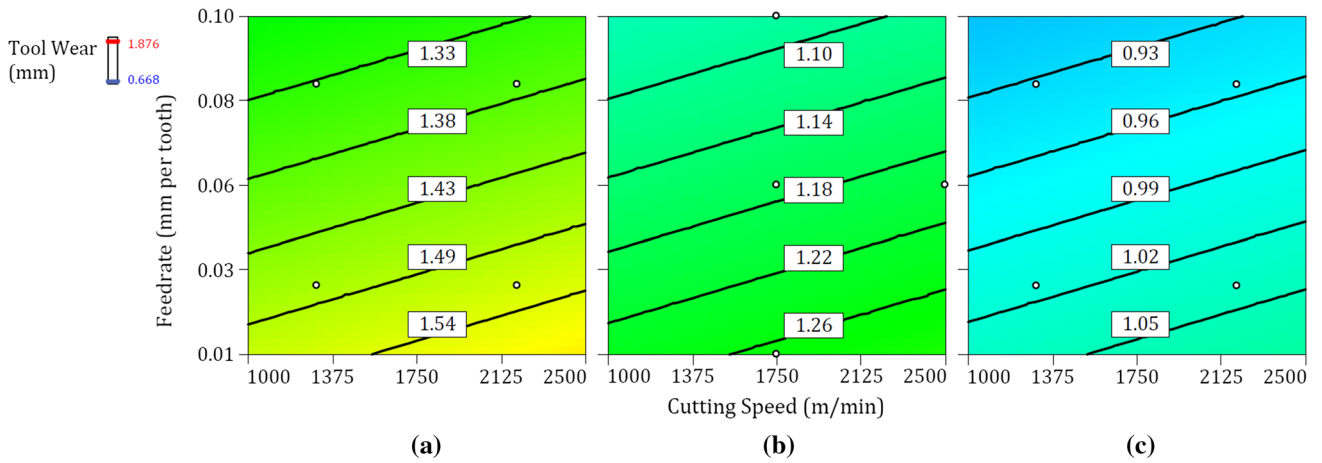

Fig. 11 Interactive effect of feed rate and cutting speed on tool wear at depth of cuts of **a** 0.6, **b** 1.13 and **c** 1.65 mm
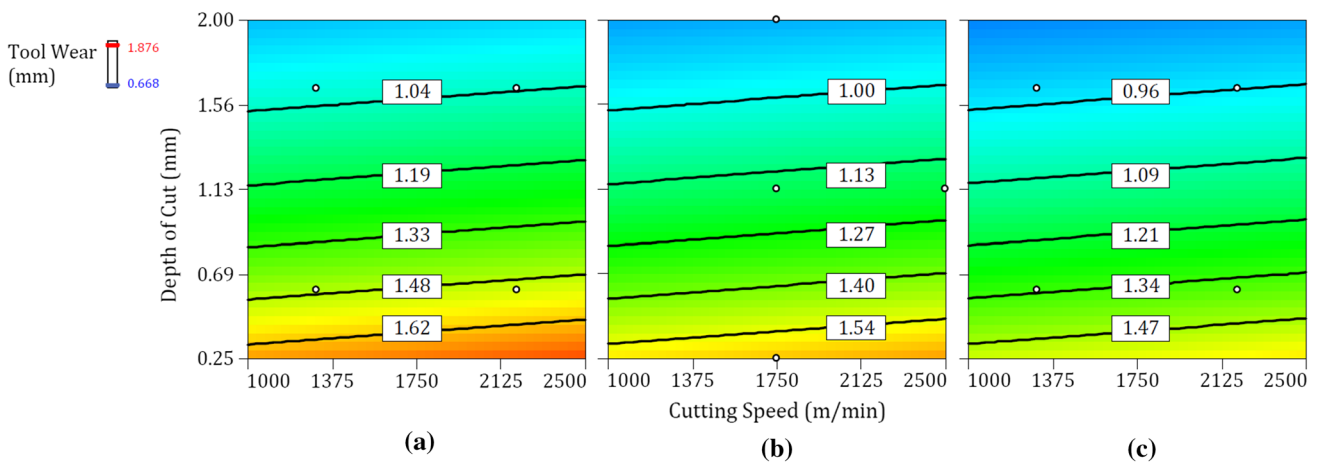

Fig. 12 Interactive effect of cutting speed and depth of cut on tool wear at feed rates of **a** 0.028, **b** 0.055 and **c** 0.082 mm/tooth

4 Conclusion

Al/SiC MMC parts were fabricated, and a set of high-speed machining experiments was conducted on the prepared parts. A deep analysis of the results of the designed experiments has been done in order to investigate the effect of different process parameters on the tool wear rates and values of the machined Al/SiC specimens. In this stage and based on the obtained results, it is safe to conclude that:

- Increasing the cutting speed does not lead to a higher tool wear value, but the rate of tool wear increases. As an instance, with increasing cutting speed from 1000 to 2500 m/min, the tool wear rate increases more than 2.5 times.
- Increasing the depth of cut and feed rate results in a faster machining process that reduces the interaction time of tool–workpiece. The reduced time decreases the final tool wear in the process, but the rate of tool wear behaves differently. As an instance, increasing depth of cut from 0.25 to 2 mm and feed rate from 0.01 to 0.1 mm/tooth increases the rate of tool wear for five and eight times, respectively.
- The optimal process parameters for achieving lower final tool wear in high-speed machining of an exact volume of material are cutting speeds higher than 1800 m/min, feed rates lower than the mean size of SiC particles (0.07 mm), depth of cuts in the range of 1–1.1 mm and utilization of a cryogenic coolant (in this case CO_2).

References

1. Clyne T, Withers P (1995) An introduction to metal matrix composites. Cambridge University Press, Cambridge
2. Geng L, Wu K (2018) Metal matrix composites. In: Composite materials engineering, vol 2, Springer, pp 305–487
3. Rawal SP (2001) Metal-matrix composites for space applications. Jom 53(4):14–17
4. Miracle D (2005) Metal matrix composites–from science to technological significance. Compos Sci Technol 65(15–16):2526–2540
5. Gireesh CH, Prasad KD, Ramji K, Vinay P (2018) Mechanical characterization of aluminium metal matrix composite reinforced with aloe vera powder. Mater Today Proc 5(2):3289–3297
6. Voyiadjis GZ, Ju J-W (2017) Inelasticity and micromechanics of metal matrix composites, vol 41. Elsevier, Amsterdam
7. Patel JA, Patel CP (2018) Development of Al–SiC MMC by bottom pouring stir casting and parametric analysis on EDM. Development 5(04):1994–2001
8. Davim JP (2008) Machining: fundamentals and recent advances. Springer, Berlin
9. Ibrahim H, Jahadakbar A, Dehghan A, Moghaddam NS, Amerinatanzi A, Elahinia M (2018) In vitro corrosion assessment of additively manufactured porous NiTi structures for bone fixation applications. Metals 8(3):164
10. Pramanik A, Zhang L, Arsecularatne J (2006) Prediction of cutting forces in machining of metal matrix composites. Int J Mach Tools Manuf 46(14):1795–1803
11. Ge YF, Xu JH, Fu YC (2011) Cutting forces when high-speed milling of SiCP/Al composites. In: Advanced materials research, Trans Tech Publ, pp 871–876
12. Heo EY, Merdol D, Altintas Y (2010) High speed pocketing strategy. CIRP J Manuf Sci Technol 3(1):1–7
13. Ke Y-L, Dong H-Y, Gang L, Zhang M (2009) Use of nitrogen gas in high-speed milling of Ti–6Al–4V. Trans Nonferrous Met Soc China 19(3):530–534
14. Velásquez JP, Tidu A, Bolle B, Chevrier P, Fundenberger JJ (2010) Sub-surface and surface analysis of high speed machined Ti–6Al–4V alloy. Mater Sci Eng A 527(10–11):2572–2578
15. Josyula SK, Narala SKR, Charan EG, Kishawy H (2016) Sustainable machining of metal matrix composites using liquid nitrogen. Procedia CIRP 40:568–573
16. Ghoreishi R, Roohi AH, Ghadikolaei AD (2018) Analysis of the influence of cutting parameters on surface roughness and cutting forces in high speed face milling of Al/SiC MMC. Mater Res Express 5(8):086521
17. Josyula SK, Narala SKR (2017) Machinability enhancement of stir cast Al–TiCp composites under cryogenic condition. Mater Manuf Process 32(15):1764–1774
18. Kumar R, Chauhan S (2015) Study on surface roughness measurement for turning of Al 7075/10/SiCp and Al 7075 hybrid composites by using response surface methodology (RSM) and artificial neural networking (ANN). Measurement 65:166–180
19. Han J, Hao X, Li L, Wu Q, He N (2017) Milling of high volume fraction SiCp/Al composites using PCD tools with different structures of tool edges and grain sizes. Int J Adv Manuf Technol 92(5–8):1875–1882
20. Bian R, He N, Li L, Zhan Z, Wu Q, Shi Z (2014) Precision milling of high volume fraction SiC p/Al composites with monocrystalline diamond end mill. Int J Adv Manuf Technol 71(1–4):411–419
21. Teng X, Chen W, Huo D, Shyha I, Lin C (2018) Comparison of cutting mechanism when machining micro and nano-particles reinforced SiC/Al metal matrix composites. Compos Struct 203:636–647
22. Vinson JR, Chou TW (1975) Composite materials and their use in structures. Halsted Press, New York
23. Ciftci I, Turker M, Seker U (2004) Evaluation of tool wear when machining SiC p-reinforced Al-2014 alloy matrix composites. Mater Des 25(3):251–255
24. Ciftci I, Turker M, Seker U (2004) Evaluation of tool wear when machining SiCp-reinforced Al-2014 alloy matrix composites. Mater Des 25(3):251–255
25. Andrewes CJ, Feng H-Y, Lau W (2000) Machining of an aluminum/SiC composite using diamond inserts. J Mater Process Technol 102(1–3):25–29
26. Dehghan Ghadikolaei A, Vahdati M (2015) Experimental study on the effect of finishing parameters on surface roughness in magneto-rheological abrasive flow finishing process. Proc Inst Mech Eng Part B J Eng Manuf 229(9):1517–1524
27. Dehghanghadikolaei A, Mohammadian B, Namdari N, Fotovvati B (2018) Abrasive machining techniques for biomedical device applications. Jupit Online J Mater Sci 5(1):1–11
28. Dehghanghadikolaei A, Ansary J, Ghoreishi R (2018) Sol-gel process applications: a mini-review. Proc Nat Rese Soc 2(1):02008

29. Lin J, Bhattacharyya D, Ferguson W (1998) Chip formation in the machining of SiC-particle-reinforced aluminium-matrix composites. Compos Sci Technol 58(2):285–291

30. Chou YK, Liu J (2005) CVD diamond tool performance in metal matrix composite machining. Surf Coat Technol 200(5):1872–1878